Review of Scientific Instruments

RESEARCH ARTICLE | MARCH 21 2023

New method for determining time constant of resistors

Yicheng Wang; Dean Jarrett; Andrew Koffman; Stephan Schlamminger

Rev Sci Instrum 94, 034711 (2023)
https://doi.org/10.1063/5.0143225

Review of Scientific Instruments | ARTICLE | scitation.org/journal/rsi

New method for determining time constant of resistors

Cite as: Rev. Sci. Instrum. 94, 034711 (2023); doi: 10.1063/5.0143225
Submitted: 20 January 2023 • Accepted: 6 March 2023 •
Published Online: 21 March 2023

View Online Export Citation CrossMark

Yicheng Wang,[a)] Dean Jarrett, Andrew Koffman, and Stephan Schlamminger

AFFILIATIONS

Quantum Measurement Division, National Institute of Standards and Technology, Gaithersburg, Maryland 20899, USA

[a)]Author to whom correspondence should be addressed: ywang@nist.gov

ABSTRACT

We report a new method for determining the time constant of ac resistors with values around 10 kΩ using a digital impedance bridge for the comparison of two nominally equal resistors. This method involves adding a probing capacitor in parallel to one of the resistors to induce a quadratic frequency dependence in the real component of the admittance ratio between the two resistors. The magnitude of this quadratic effect is proportional to the self-capacitance of the unperturbed resistor, enabling us to determine its value and the associated time constant with an estimated standard uncertainty ($k = 1$) of 0.02 pF and 0.2 ns, respectively.

Published by AIP Publishing. https://doi.org/10.1063/5.0143225

I. INTRODUCTION

An ac resistor can be modeled by a lumped circuit of a resistance R in series with an inductance L, and a self-capacitance C across the whole. The phase angle between the applied voltage and the current is, then, $\omega(L/R - RC) \equiv \omega\tau$, where τ is the time constant.[1] Some precision resistors have been designed and fabricated to minimize L and C, achieving a typical inductance of 0.08 μH and a capacitance of 0.5 pF.[2] For such resistors around 10 kΩ, which is the focus of the present work, the contribution of L to the phase angle and the time constant can further be considered negligible and the ac resistor can be represented by a parallel RC circuit. The accurate determination of the time constant is important in many applications of precision resistors.

The phase angles of ac resistors are most readily determined in reference to a standard resistor of known phase angle. A commercial quadrifilar resistor of 10 kΩ has been used as a reference to determine the time constants of custom-developed metal-foil resistors.[3] The calculated self-capacitance of a typical quadrifilar resistor, however, has a standard uncertainty on the order of 0.1 pF.[4,5] The time constants of metal-film resistors have been determined more accurately by comparing two resistors constructed with geometrical similarity but different values of resistance using a sophisticated four-terminal-pair (4TP) bridge.[6] A simpler quadrature bridge has been reported to determine the time constants of standard ac resistors in reference to the known dissipation factor of a capacitor, achieving a standard uncertainty of 8 ns.[7] A gas-filled 1 nF standard capacitor has also been used to compare with a stable 1 MΩ ac resistor with a digital multi-frequency method, simultaneously determining the dissipation factor of the capacitor and of the time constant of the resistor.[8]

We report a new method here for determining the time constant of ac resistors around 10 kΩ with a small self-capacitance. We recognize that by adding a probing fused-silica capacitor with an admittance $j\omega C$ and a negligible dissipation factor, in parallel, to a resistor with an admittance Y_1 in comparison with another resistor with an admittance Y_2, we would only change the imaginary part of the admittance ratio, $(Y_1 + j\omega C)/Y_2$, if the two resistors were pure, as illustrated in Fig. 1(a). In reality, however, the measurement axis defined by Y_2 is slightly tilted from the reference axis for the conductances of Y_1 and Y_2, as shown in Fig. 1(b), and the probing capacitor will also induce a small change in the real part of the admittance ratio. This induced change allows us to measure the self-capacitance of Y_2, analogous to the more thoroughly studied Abbe error that occurs in displacement measurements when the measurement axis deviates slightly from the reference axis in parallel.[9]

II. BRIDGE SETUP

The digital impedance bridge, shown in Fig. 2, is designed for the comparison of two nominally equal resistors.[10] Here, we focus on two 4TP Vishay[17] resistors, Z_1 and Z_2 (with their admittances

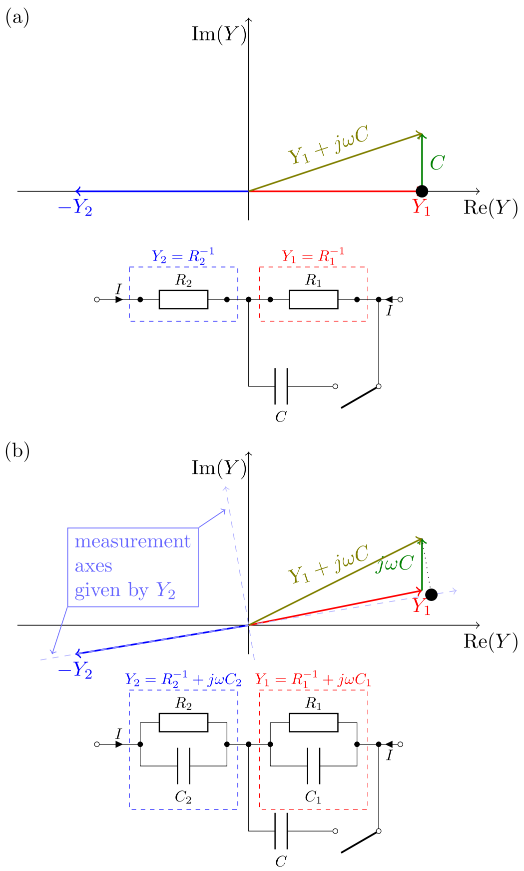

FIG. 1. Schematic of the probing method: (a) for pure Y_1 and Y_2, a probing capacitor does not disturb the real part of the admittance ratio; (b) for real Y_1 and Y_2, a probing capacitor induces a change in the real part because the measurement axis for the ratio is tilted.

denoted Y_1 and Y_2, respectively), each with a nominal value of 12 906 Ω in an air bath at 23 °C. The bridge was excited through a 1:1 transformer, driven by a Keysight 33500B waveform generator, S_1. The generator was set to produce a two-tone sinusoidal waveform in its built-in combination mode, applying root mean square (rms) voltages of 0.1 V to the high current ports of the resistors with the two frequencies in the range from 160 Hz to 5 kHz. With the two-tone excitation scheme, the complex impedance ratio was measured at two frequencies simultaneously. After one such measurement, one of the two frequencies was changed and another two points were obtained, and so forth. The common pairwise point can be used to reject the drift that can occur when the laboratory temperature changes excessively such that the stabilities of the resistors are impacted. The bridge was dynamically balanced at each frequency with coaxial injection through a 10 000:1 injection transformer inserted into the lower excitation arm using another synchronized 33500B generator, S_2. An external time base was used for both generators with their 10 MHz reference signal locked to the global positioning system.

The low potential ports of the 4TP resistors were connected together through a combining network consisting of two closely matched resistors of 1 kΩ (Z_A and Z_B). The effectiveness of this combining network was verified by inserting a 10 Ω resistor between the low current ports of Z_1 and Z_2 and detecting no change larger than the type A uncertainty of the bridge. A current amplifier (Femto DLPCA-200) with a transimpedance of Z_3 was used to detect the bridge error voltage.

The voltages across Z_1, Z_2, and Z_3, namely V_1, V_2, and V_3, respectively, are digitized synchronously using a Keysight DAQM909A[13] and demodulated independently at each excitation frequency, with their sine-fitting complex amplitude denoted by U_1, U_2, and U_3, respectively. The bridge is dynamically balanced, using a simple proportional-integral feedback algorithm, through the coaxial injection S_2 such that $U_3 = 0$, statistically. Then, the balance equation is

$$\frac{Y_1}{Y_2} \equiv 1 + \alpha + j\beta = -\frac{U_2}{U_1}, \tag{1}$$

where α and β represent the real and imaginary parts, respectively, of the deviation from the nominal admittance ratio of 1.

III. TEST RESULTS AND DISCUSSIONS

The resolution of the digitizer for the measurements of α and β is about 2×10^{-7} with a single sampling record, independent of the frequency in the range from 160 Hz to 5 kHz. Lower type-A uncertainty was achieved through averaging. Shown in Fig. 3 are the typical Allan deviations of α and β measured at 5 kHz as a function of averaging time. Both decrease along a straight line in the log–log plot, with their slopes consistent with averaging over white noise. The baseline α and β, measured over the test frequency range before adding a probing capacitor, are shown in Fig. 4. The averaging time for each data point was ~3 h, guided by the Allan deviations. To understand the linear frequency dependence of α, which has previously been observed in similar Vishay resistors,[14] we recognize that the Vishay resistors are metal foils attached to ceramic substrates and are hermetically sealed in oil filled cans. The equivalent parallel capacitance has dissipation in the substrate and the oil that can be represented by its dissipation factor, tanδ. The admittances of the two resistors are

$$Y_1 = \frac{1}{R_1} + j\omega C_1(1 - j\tan\delta_1), \tag{2}$$

$$Y_2 = \frac{1}{R_2} + j\omega C_2(1 - j\tan\delta_2). \tag{3}$$

From the definition of α and β, we have (neglecting the higher-order frequency dependent terms)

$$\alpha = \alpha_o + \omega(R_1C_1\tan\delta_1 - R_2C_2\tan\delta_2) + \omega^2(R_1R_2C_1C_2 - R_2^2C_2^2), \tag{4}$$

$$\beta = \omega(R_1C_1 - R_2C_2), \tag{5}$$

where $\alpha_o = R_2/R_1 - 1$ is the dc offset of the admittance ratio. The apparent linear frequency dependence of α in Fig. 4 indicates that

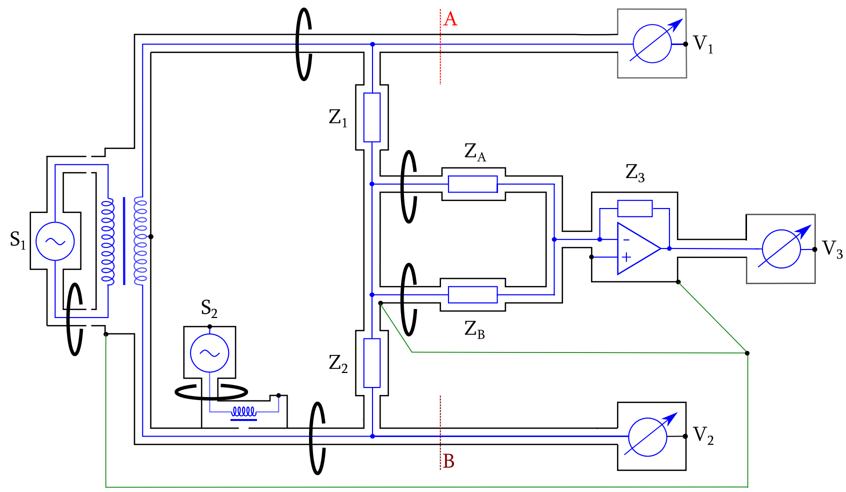

FIG. 2. Schematic of digital impedance bridge for the comparison of two nominally equal resistors, Z_1 and Z_2 (12 906 Ω). S_1 and S_2 are waveform generators. The bridge is excited through a 1:1 transformer with two mixed frequencies ranging from 160 Hz to 5 kHz, each with an amplitude of 0.1 V. V_1, V_2, and V_3 are ac voltmeters. V_1 and V_2 are connected to the high-potential ports (A and B) and are periodically interchanged to minimize the effect of their gain drift. S_2 is adjusted such that V_3 is nominally 0. A combining network consisting of two closely matched resistors of 1 kΩ (Z_A and Z_B) is added to the low potential leads, and the bridge error is detected through a current amplifier with a feedback resistor Z_3. A single conductor (green) is added to connect the selected points of the coaxial outer conductors to improve the current equalization effect of the indicated coaxial chokes (black).[11,12]

$\tan\delta_1$ and $\tan\delta_2$ are approximately constant. The linear frequency dependence of β indicates that $C_2 - C_1 = 0.12$ pF.

After we add a pure capacitor C in parallel to Y_1, it is straightforward to derive that we introduce additional frequency dependent terms in the admittance ratio,

$$\Delta\alpha = \omega^2 R_1 R_2 C C_2, \tag{6}$$

$$\Delta\beta = \omega R_1 C. \tag{7}$$

We used a programmable fused-silica capacitor[15,16] with a negligible dissipation factor ($\tan\delta < 10^{-6}$) as the probing C. With its value set equal to 8.887 pF, shown in Figs. 5(a) and 5(b) are the measured results of $\Delta\alpha$ and $\Delta\beta$, respectively, as a function of frequency from 160 Hz to 5 kHz. The slope of the linear frequency dependence of $\Delta\beta$ is consistent with the known value of C. The observed quadratic frequency dependence is consistent with Eq. (6), enabling us to determine C_2. Shown in Fig. 6(a) are $\Delta\alpha$, together with the

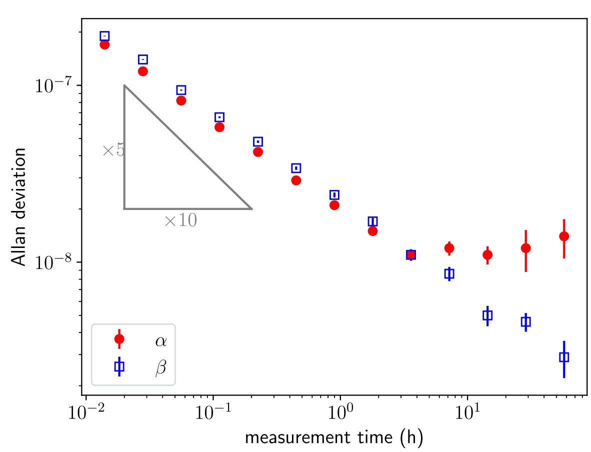

FIG. 3. Solid circles and open squares give the Allan deviations of α and β measured at 5 kHz as a function of measurement time. Error bars are $1-\sigma$ standard deviation of the Allan deviation. A triangle is added to indicate that the Allan deviations decrease along straight lines with their slopes approximately equal to −1/2 in the log–log plot.

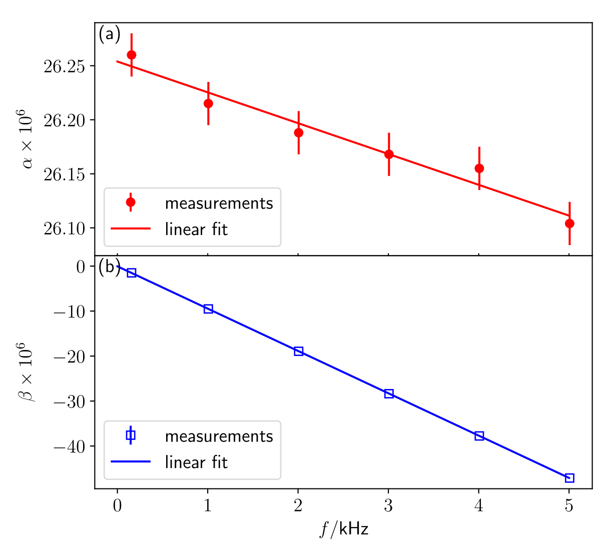

FIG. 4. Baseline α (a) and β (b), measured before adding a probing capacitor, as a function of frequency. Error bars are $1-\sigma$ standard deviation.

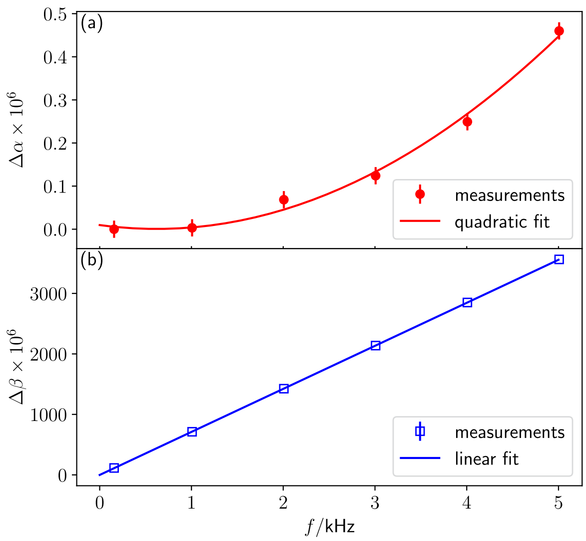

FIG. 5. Changes in α and β denoted as $\Delta\alpha$ (a) and $\Delta\beta$ (b) after adding a probing capacitor of C = 8.887 pF in parallel to Z_1 as a function of frequency. Error bars are $1 - \sigma$ standard deviation.

residuals of a linear fit in Fig. 6(b), as a function of C from 0 to 8.887 pF.

According to Eq. (6), the induced $\Delta\alpha$ for a given C_2 is proportional to ω^2 and C. The choices of these parameters are limited not only by the range of the bridge injection circuit (Fig. 2) but also by the uncertainty contributions that are related to the parameters. The value of the self-capacitance of Z_2 is determined from the results obtained at 5 kHz and C = 8.887 pF and is found to be C_2 = 0.32 pF, and the associated measurement uncertainty is directly

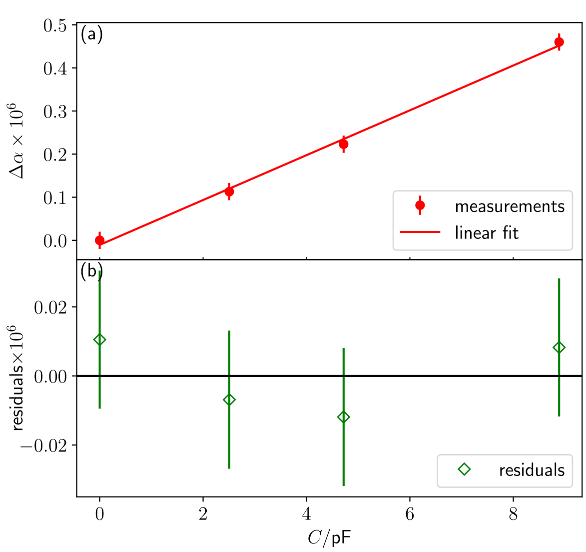

FIG. 6. Measured change in α, $\Delta\alpha$ (a), at 5 kHz as a function of the parallel capacitance C added to Z_1. A linear dependence is found. The residuals from a straight line fit are shown in the bottom panel (b). Error bars are $1 - \sigma$ standard deviation.

TABLE I. Uncertainty budget (k = 1) of the determination of $\Delta\alpha$.

	Standard uncertainty ($\times 10^{-6}$)
Type A uncertainty of $\Delta\alpha$	0.015
Nonlinearity in measurement of $\Delta\alpha$	0.01
Contribution $\Delta\beta$ to $\Delta\alpha$ due to phase error	0.003
Combined standard uncertainty	0.02

proportional to the measurement uncertainty of $\Delta\alpha$. The uncertainty budget for the combined standard uncertainty of $\Delta\alpha$ is shown in Table I. The type A uncertainty of $\Delta\alpha$ is the dominant component. The nonlinearity error in the measurement of $\Delta\alpha$ was estimated from the slight change in the amplitude ratio of U_1 and U_2 after adding the probing C. The nonlinearity error is expected to increase if the proposed method is used for a different resistance ratio. The phase error between the two detected voltages was found to be about 6×10^{-7}, determined at 0° by connecting the two digitizer channels to the same voltage source and at 180° by interchanging Z_1 and Z_2 in the bridge measurements. The uncertainty contribution of $\Delta\beta$ to $\Delta\alpha$ due to the phase error was then estimated. The crosstalk between the digitizer channels cancels out because the bridge is symmetrical. The relative standard uncertainty of C_2 equals that of $\Delta\alpha$ because the relative uncertainty contributions of ω^2, C, R_1, and R_2 are negligible. The absolute standard uncertainty (k = 1) of C_2 is then 0.02 pF, and the associated time constant of Z_2 is −4.1 ns with a corresponding standard uncertainty (k = 1) of 0.2 ns.

While the determined value of C_2 cannot be directly verified, the capacitive component of Y_2 can be altered by adding a small capacitor, ΔC_2, in parallel, which can be determined through a difference measurement. Using a variable air-gap capacitor for ΔC_2, the value determined with the present method is shown in Fig. 7 as a function of its known value measured by a precision capacitance bridge. They agree within the estimated standard uncertainty.

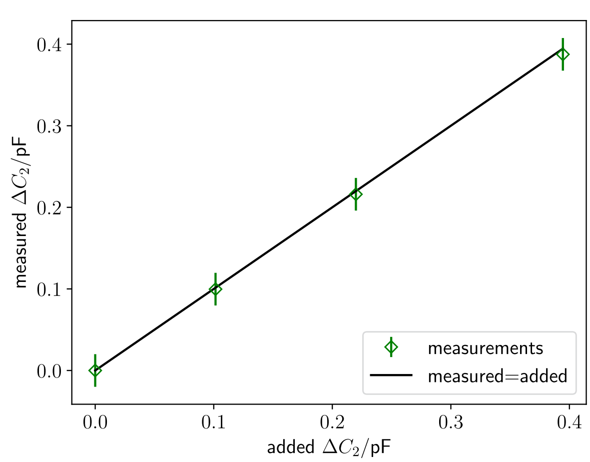

FIG. 7. Measured ΔC_2, according to Eq. (6), as a function of its known value, measured by a precision capacitance bridge. The solid black line is not a fit to the data but indicates the locations where the measured values agree with the added ΔC_2. Error bars are the measurement uncertainty of the digital bridge.

IV. CONCLUSION

We evaluated a new method for determining the time constant of ac resistors around 10 kΩ using a digital impedance bridge for the comparison of two nominally equal resistors. By adding a probing capacitor, in parallel, to one of the resistors, we induce a quadratic frequency dependence in the real component of the admittance ratio, taking advantage of the excellent phase control and stability of the digital bridge. The magnitude of this induced effect is proportional to the self-capacitance of the unperturbed resistor, enabling us to determine its value and the associated time constant with the estimated standard uncertainty ($k = 1$) of 0.02 pF and 0.2 ns, respectively.

AUTHOR DECLARATIONS

Conflict of Interest

The authors have no conflicts to disclose.

Author Contributions

Yicheng Wang: Conceptualization (lead); Data curation (equal); Resources (equal); Software (equal); Writing – original draft (lead); Writing – review & editing (equal). **Dean Jarrett**: Resources (equal); Writing – review & editing (equal). **Andrew Koffman**: Resources (equal); Writing – review & editing (equal). **Stephan Schlamminger**: Data curation (equal); Software (equal); Writing – review & editing (equal).

DATA AVAILABILITY

The datasets generated during and/or analyzed during the current study are available from the corresponding author on reasonable request.

REFERENCES

[1] G. H. Rayner and L. H. Ford, "The a.c. properties of resistors and potential dividers at power and audio frequencies, and their measurement," J. Sci. Instrum. **34**, 190 (1957).

[2] See https://foilresistors.com/docs/63120/hzseries.pdf for HZ Series, Vishay Precision Group.

[3] A. Domae, T. Oe, M. Kumagai, M. Zama, and N.-h. Kaneko, "Characterization of 100-Ω metal foil standard resistors," IEEE Trans. Instrum. Meas. **62**(6), 1776–1782 (2013).

[4] B. P. Kibble, A. Hartland, and S. W. Chua, "Calculable AC/DC resistor for ac quantized Hall resistance experiments," in *BEMC 97 8th International Conference on Electromagnetic Measurement Digest* (National Physical Laboratory, Teddington, 1997), http://eprintspublications.npl.co.uk/id/eprint/881.

[5] J. Bohácek and B. M. Wood, "Octofilar resistors with calculable frequency dependence," Metrologia **38**, 241 (2001).

[6] A. M. Thompson, "Standards for the measurement of the phase angles of resistors," Proc. Inst. Electr. Eng. **122**(5), 576–578 (1975).

[7] L. L. Jian Feng, L. Shi, H. Shi, Y. Pan, and B. Zhou, "Measurement of the time constant of four-terminal resistor based on dissipation factor of capacitor," in *Conference on Precision Electromagnetic Measurements* (IEEE, 2016), pp. 1–2.

[8] G. Ramm and H. Moser, "New multifrequency method for the determination of the dissipation factor of capacitors and of the time constant of resistors," IEEE Trans. Instrum. Meas. **54**(2), 521–524 (2005).

[9] R. Köning, J. Flügge, and H. Bosse, "A method for the in situ determination of Abbe errors and their correction," Meas. Sci. Technol. **18**, 476–481 (2007).

[10] Y. Wang, A. Hafner, D. Jarrett, A. Koffman, and S. Schlamminger, "A two-tone digital impedance bridge," in *Conference on Precision Electromagnetic Measurements* (IEEE, 2022), pp. 1–2.

[11] D. N. Homan, "Applications of coaxial chokes to A-C bridge circuits," J. Res. Natl. Bur. Stand. **72C**, 161–165 (1968).

[12] S. A. Awan, J. Schurr, and B. P. Kibble, *Coaxial Electrical Circuits for Interference-Free Measurements*, IET Electrical Measurement Series (Institution of Engineering and Technology, London, 2011).

[13] M. Feige, S. Schlamminger, A. D. Koffman, D. G. Jarrett, S. Payagala, A. Panna, B. C. Waltrip, M. Berilla, F. Seifert, and Y. Wang, "Comparison of a 100-pF capacitor with a 12 906-Ω resistor using a digital impedance bridge," IEEE Trans. Instrum. Meas. **71**, 1500407 (2022).

[14] J. Schurr, N. Fletcher, P. Gournay, O. Thévenot, F. Overney, L. Johnson, R. Xie, and E. Dierikx, "Final report of the supplementary comparison EURAMET.EM-S31 comparison of capacitance and capacitance ratio," Metrologia, **54**, 01016 (2017).

[15] Y. Wang and L. Lee, "A digitally programmable capacitance standard," Rev. Sci. Instrum. **75**, 1158 (2004).

[16] Y. Wang, A. D. Koffman, and G. J. FitzPatrick, "Dissipation factors of fused-silica capacitors in the audio frequency range," IEEE Trans. Instrum. Meas. **56**, 624 (2007).

[17] Certain commercial equipment, instruments, or materials are identified in this paper to foster understanding. Such an identification does not imply recommendation or endorsement by the National Institute of Standards and Technology, nor does it imply that the materials or equipment identified is necessarily the best available for the purpose.